Energy Reports 8 (2022) 8333–8345

Contents lists available at ScienceDirect

Energy Reports

journal homepage: www.elsevier.com/locate/egyr

Research paper

Modelling and prediction approach for engine performance and exhaust emission based on artificial intelligence of *sterculia foetida* biodiesel

A.H. Sebayang [a], Jassinnee Milano [b,c,*], Abd Halim Shamsuddin [b,c,*], Munawar Alfansuri [d], A.S. Silitonga [a,e,**], Fitranto Kusumo [b,c], Rico Aditia Prahmana [f], H. Fayaz [g], M.F.M.A. Zamri [b,c]

[a] *Department of Mechanical Engineering, Politeknik Negeri Medan, 20155 Medan, Indonesia*
[b] *Institute of Sustainable Energy, Universiti Tenaga Nasional, Kajang, Selangor, Malaysia*
[c] *Department of Mechanical Engineering, College of Engineering, Universiti Tenaga Nasional, Kajang, Selangor, Malaysia*
[d] *Department of Mechanical Engineering, Faculty of Engineering, Universitas Muhammadiyah Sumatera Utara, 20238 Medan, Indonesia*
[e] *Centre for Technology in Water and Wastewater, School of Civil and Environmental Engineering, Faculty of Engineering and Information Technology, University of Technology Sydney, NSW 2007, Australia*
[f] *Program Study of Mechanical Engineering, Department of Production and Industrial Technology, Institut Teknologi Sumatera, 3536, Lampung, Indonesia*
[g] *Modelling Evolutionary Algorithms Simulation and Artificial Intelligence, Faculty of Electrical and electronics Engineering, Ton Duc Thang Unviversity, Ho Chi Minh City, Viet Nam*

ARTICLE INFO

Article history:
Received 21 January 2022
Received in revised form 29 April 2022
Accepted 17 June 2022
Available online xxxx

Keywords:
Biodiesel
Diesel engine
Emission characteristic
Engine performance
Sterculia foetida

ABSTRACT

Sterculia foetida derived biodiesel is a potential fuel for a diesel engine. The *Sterculia foetida* biodiesel required a pre-refining process called degumming and an acid pretreatment process before converting them to methyl ester using the transesterification process. This study blended fuel from *Sterculia foetida* biodiesel and diesel with different volume ratios (5% to 30% of biodiesel blend with 95% to 70% diesel fuel). *Sterculia foetida* biodiesel and blended fuels met the ASTM D6751 and EN 14214 standards. The blended fuel is examined to obtain its influences on the performance and emission when operating at a diesel engine (1300 rpm to 2400 rpm). From the outcome, the engine performance of the SFB5 blend shows better performance than diesel fuel in terms of BTE (28.84%) and BSFC (5.86%). Artificial neural networks and extreme learning machines were employed to predict engine performance and exhaust emissions. The developed models gave excellent results, where the coefficient of determination is more than 99% and 98% for BSFC and BTE, respectively. When the engine is operated with SFB5, there is a significant reduction in CO, HC, and smoke opacity emissions by 8.26%, 2.08%, and 3.08%, respectively, and at the same time, an increase in CO_2 by 3.53% and NO_X by 22.39%. The comparison is made with diesel fuel. The extreme learning machine modelling is powerful for predicting engine performance and exhaust emission compared to artificial neural networks in terms of prediction accuracy. *Sterculia foetida* biodiesel–diesel blends of 5% show its capability to replace diesel fuel by providing engine peak performance than diesel fuel.

1. Introduction

Diesel engines are widely used in power generation and have wide applications due to its high reliability and durability than petrol engines and gas turbines (Chen et al., 2019b). However, the pollution derived from the diesel engine application has caused severe pollution to the environment through greenhouse gas emissions such as carbon dioxide (CO_2), carbon monoxide (CO), nitrogen oxides (NO_x), unburned hydrocarbons (UHC) and particulate matter (PM) (Adam et al., 2018; Goh et al., 2020). This long-term exposure of diesel consumption has gradually affecting

* Corresponding authors at: Institute of Sustainable Energy, Universiti Tenaga Nasional, Kajang, Selangor, Malaysia.
** Corresponding author at: Department of Mechanical Engineering, Politeknik Negeri Medan, 20155 Medan, Indonesia.
E-mail addresses: jassinneemilano.jm@gmail.com, jassinneemilano@hotmail.com (J. Milano), abdhalim@uniten.edu.my (A.H. Shamsuddin), ardinsu@yahoo.co.id, arridinasusan.silitonga@uts.edu.au, arridina@polmed.ac.id (A.S. Silitonga).

https://doi.org/10.1016/j.egyr.2022.06.052

the global ecology through the air pollutions and global warming. Alternatively, biodiesel has worked as an option fuel to substitute diesel usage (Tulashie et al., 2018; Mofijur et al., 2013). Several researchers such as Yesilyurt (2019), Vijay Kumar et al. (2018) and Ashok et al. (2018) have blended biodiesel with diesel fuel and assessed it in a direct-injection engine without modifying the engine. Blending conventional diesel with biodiesel has been shown to minimise smoke opacity, particulates, UHC, CO_2 and CO, but NO_x levels have risen significantly. No serious engine problems were identified during a diesel engine's performance, durability test and tribological analysis powered with biodiesel–diesel blending (Milano et al., 2022, 2021; Dharma et al., 2019). Furthermore, the blending fuel has improved brake thermal efficiency and lowered NOx emission when compared to conventional diesel and hydrocarbon and CO emissions was rose slightly (Ilkılıç et al., 2011). Nevertheless, the usage of biodiesel fuel requires experimental and numerical testing of their influences on engine performance and emission exhaust. These requires numberous of experimental and testing that were time consumed and costly. Instead, modelling simulations are gaining more attention as it very useful to exploit and handle information for biodiesel–bioethanol–diesel performance parameter studies which influence engine operating conditions and emissions exhaust.

Several typical techniques of modelling simulations with the ability to predict the data accurately within the entire domain of experimental study were used artificial intelligence (AI) such as artificial neural network (ANN) and extreme learning machine (ELM) as a robust system identification tool (Lešnik et al., 2014; Oğuz et al., 2010). AI-based engine performance and emission exhaust modelling is a fast adaptive model system that having inherent robustness to accommodate data with appreciable degrees of observation uncertainties which allowing prediction and interpolations for control results (Tasdemir et al., 2011; Roy et al., 2014). The ANN is a mathematical model to solve a wide variety of problems in science and engineering, such as biofuel production, heat transfer and engine performance tests (Hulwan and Joshi, 2011). A well-trained ANN can be used as a predictive model for a specific application, a data-processing system inspired by the biological neural system (Oğuz et al., 2010). The predictive ability of an ANN results from the training on experimental data and validation by independent data. An ANN can re-learn to improve its performance if new data are available (Canakci et al., 2009). The literature studies showed that ANN has a powerful modelling technique to predict engine performance and exhaust emissions including the thermal contact conductance in the exhaust valve (Tasdemir et al., 2011; Roy et al., 2014; Ghobadian et al., 2009; Goudarzi et al., 2015). Furthermore, ANN could also estimating the periodic contact heat transfer in the exhaust valve. As reported by Mohamed Ismail et al. (2012), ANN was used to predict emission exhaust such as CO, CO_2 and nitrogen monoxide (NO) respectively. As observed ANN provides good level of accuracy in modelling the emission concentration of CO, CO_2, and NO_x with the average correlation coefficient is 0.98 respectively.

Alternatively, ELM is also mathematical modelling that actively been used due to its strong generalisation performance and its straightforward solution (Huang et al., 2006). It is a single-hidden layer feed-forward neural network where the hidden layer parameters are initialised randomly. Moreover, ELM can calculate the output weights analytically with extremely fast learning speed and better generalisation capability (Wong et al., 2013, 2015a). As studied by Mozaffari and Azad (2014), ELM was used to identify the exhaust gas temperature (T_{exh}) and the engine-out hydrocarbon emission (H_{Craw}) of a cold start phenomenon by obtaining the mean absolute percentage error (MAPE) of sparse Bayesian extreme learning machine (SBELM) is 0.08%. Similarly, Wong et al. (2015a) compared two mathematical modellings such as ELM and least-squares support vector machine (LS-SVM), to determine the optimal biodiesel ratio to reduce exhaust emissions for various engine operating conditions. The result showed the MAPE test data sets for K-ELM and LS-SVM is 2.97% and 3.06%, indicating that K-ELM is 0.09% better than LS-SVM. Besides, K-ELM is also superior in training time and executive time for fast learning speed and short computation time.

Nevertheless, the prediction modelling is a complicated that requires extra computational resources and high computational power (Chen et al., 2019a). Unlike traditional learning algorithms, the ELM tends to reach the slightest training error and the smallest norm of output weights compared to the conventional learning algorithms, making the regression performance better. The essence of ELM is that the hidden layer parameters can be independent of training samples, and the hidden layer of the generalised SLFNs need not be tuned (Wong et al., 2015b). Therefore random sub-sampling cross-validation was adopted in this study to evaluate the performance of the modelling methods for ELM (Wong et al., 2013, 2015a). In this attempt, ANN and ELM mathematical modelling were adopted to predict engine performance and study the exhaust emission parameters. Biodiesel derived from *Sterculia foetida* oil was used for blending with diesel. This research studies and evaluates the main properties of the biodiesel–diesel blends then compares them with diesel fuel as baseline (reference). The blending of various volume ratios of biodiesel–diesel was performed to determine the blended fuel's optimal properties. The aim of blending biodiesel with diesel was to increase the oxygen content of the blended fuel while keeping other properties such as viscosity, oxidation stability and calorific value within the permissible range stipulated in ASTM and EN limits. Besides, this research was performed as a comparative of ANN and ELM modelling to evaluate the visibility of *Sterculia foetida* biodiesel as a sustainable feedstock. The findings is to solve the approximation, optimisation and the control problems function in biodiesel research using ANN and ELM as a modelling system.

2. Materials and methods

2.1. Materials

Sterculia foetida oil was purchased from West Java, Indonesia. The chemicals used for biodiesel production and properties identification were phosphoric acid (H_3PO_4, purity: 85%), sulphuric acid (H_2SO_4, purity: >98.9%), sodium hydroxide (NaOH, purity: 99%), methanol (CH_3OH, purity: 99.9%), sodium sulfate (Na_2SO_4, purity: >99%), FAME mix ($C_8 - C_{24}$, purity: >99.5%), and methyl nonadecanoate (C_{19}, purity: >99.5%). Petroleum pure diesel was purchased from Hakita Sdn Bhd, at Kuala Lumpur, Malaysia.

2.2. Biodiesel production

The *Sterculia foetida* biodiesel is produced through three process (degumming, acid-pretreatment, and transesterification processes). Three-process was performed in a double jacketed reactor at Biofuel Laboratory, Level 3, Block M, Faculty of Mechanical Engineering, University Malaya. For the degumming process, *sterculia foetida* crude oil was mixed with 0.5% vol. of phosphoric acid with 20% concentration at temperature of 60 °C for 30 min. Density separation was done by placing the mixture in a separation funnel, where the gum and impurities were found at the bottom. Then the oil was washed with distilled water several times and dried in a rotary evaporator at 60 °C for 30 min. Then

the degummed oil is ready for the next process, which is called esterification.

The esterification process required mixing degummed oil with methanol/oil molar ratio of 10:1, 1% vol. of sulphuric acid, stirring speed of 1200 rpm, reaction temperature set at 60 °C, and reaction time are 180 min. Separation was performed in a separation funnel. Two distinct layers were observed from the separation funnel. The upper layer consisted of methanol, while the bottom layer was esterified *sterculia foetida* oil. Then collect the esterified *sterculia foetida* oil for the transesterification process.

The transesterification process was performed by mixing esterified oil with methanol/oil molar ratio of 10:1, 1% vol. of sodium hydroxide, stirring speed of 1200 rpm, reaction temperature set at 50 °C, and duration of reaction was 120 min. There are also two distinct layers formed in the separation funnel. The top layer consists of fatty acid methyl ester, while the bottom consists of methanol, glycerol and other impurities. The fatty acid methyl ester was collected for the purification and drying process. The fatty acid methyl ester was washed with distilled water several times to remove the remaining impurities and glycerol. Then the methyl ester was dried using a rotary evaporator for 60 min at 60 °C. Then sodium sulfate was added to dried fatty acid methyl ester to ensure a 100% water-free product.

2.3. Blending

The preparation of biodiesel diesel blends was performed at 26 °C using a beaker glass. The agitation speed was set at 2000 rpm, to ensure homogeneity between biodiesel and diesel. SFB5, SFB10, SFB20, and SFB30 blends were obtained by mixing diesel and biodiesel in the following proportions by volume: 5% biodiesel with 95% diesel, 10% biodiesel with 90% diesel, 20% biodiesel with 80% diesel, 30% biodiesel with 70% diesel, respectively.

2.4. Physicochemical properties of fuel

We examined and analysed the physicochemical properties of the *sterculia foetida* crude oil, biodiesel, and biodiesel blend. The fuel properties were measured based on the fuel specification stipulated in ASTM D 6751 and EN 14214 standard. The tested properties were viscosity kinematic at 40 °C, density at 15 °C, acid value, calorific value, flash point, pour point, cloud point, and oxidation stability at 110 °C. The results is shown in Table 4. All properties testing was performed in Energy Efficiency Laboratory, Level 2, Block M, Faculty of Mechanical Engineering, University Malaya.

2.5. Engine evaluation

In a diesel engine, the performance and emissions of *Sterculia foetida* biodiesel–diesel blends were studied. The engine performance test was performed in Heat engine laboratory, Level 1, Block M, Faculty of Mechanical Engineering. For the engine evaluation analysis, the four mixed fuels were acquired and then compared to diesel (baseline/reference). The experimental setup for the engine's performance and emission test was shown in Fig. 1. In addition, a gas exhaust analyser was used to detect the exhaust emissions such as NO_x, CO, CO_2 and smoke opacity. The specification of the diesel engine used in this study was tabulated in Table 1. An eddy current dynamometer and electronic data collecting devices were used in conjunction with the engine. The test began with diesel to warm up the engine for 15 min. The engine performance and emission produced will be recorded after the engine stabilises. Then, the diesel engine is supplied with biodiesel blends (SFB5, SFB10, SFB20, and SFB30). The engine will idle for another 15 min with the blended fuels before the next experimental recording. All engine parameters were measured after, including torque, power, specific fuel consumption, and exhaust temperature. The speed was measured at 100 rpm intervals from 1300 to 2400 rpm. The BOSCH BEA 150 analyser was used to measure emissions and smoke opacity after the engine had reached a stable functioning condition. The exhaust emissions were measured using a sensor filter by placing it at the exhaust pipe. Table 2 shows the specification of gas analyser. The results was tripleted and the average was calculated.

Table 1
Technical specification of the test engine.

Type	TF 120 M Yanmar
Injection system	Direct injection
Cylinder number	1
Cylinder bore × stroke volume	92 mm × 96 mm
Displacement	0.638 L
Compression ratio	17.7:1
Maximum power	7.7 kW
Maximum engine speed	2400 rpm
Cooling system	Water cooling
Injection timing	17.0 bTDC
Injection pressure	200 kg/cm^2

Table 2
Technical data and specification of the gas analyser device.

Technical data		
Exhaust component	Measurement range	Resolution
CO	0.000–10.00% vol.	0.001% vol.
CO_2	0.00–18.00% vol.	0.01% vol.
O_2	0.00–22.00% vol.	0.01% vol.
NO	0–5000 ppm vol.	≤1 ppm vol.
Smoke opacity meter module		
Measured quantity	Measurement range	Resolution
Degree of opacity	0%–100%	0.1%
Oil temperature		
Measured quantity	Measurement range	Resolution
Temperature	−20–+150 °C	0.16 °C

2.6. ANN Modelling

2.6.1. Normalisation

The training model dataset was normalised so that the values are within the range of [0,1] using the following equation:

$$N(v) = e_i = \frac{(e_i - E_{min})}{(E_{max} - E_{min})} \quad (1)$$

where: e_i represents the normalised parameter, whereas E_{max} and E_{min} represent the upper and lower bound, respectively. Since all of the values in the training process are normalised, the values predicted by the models need to be denormalised using the inverse of Eq. (1).

2.6.2. ANN generalisation

MATLAB 7.10.0 was used to train the developed back-propagation of ANN to generate the neural network. In this study, a three-layer feed-forward was used. The hyperbolic tangent sigmoid (TANSIG) transfer function was used from input to hidden layer, while the PURELIN transfer function was used from hidden layer to output. The tan sig and the pure lin transfer function are expressed as Eqs. (2) and (3) as below:

$$\tan sig\,(x) = \frac{2}{\left(1 + e^{-2x}\right)} - 1 \quad (2)$$

$$A = purelin\,(x) = x \quad (3)$$

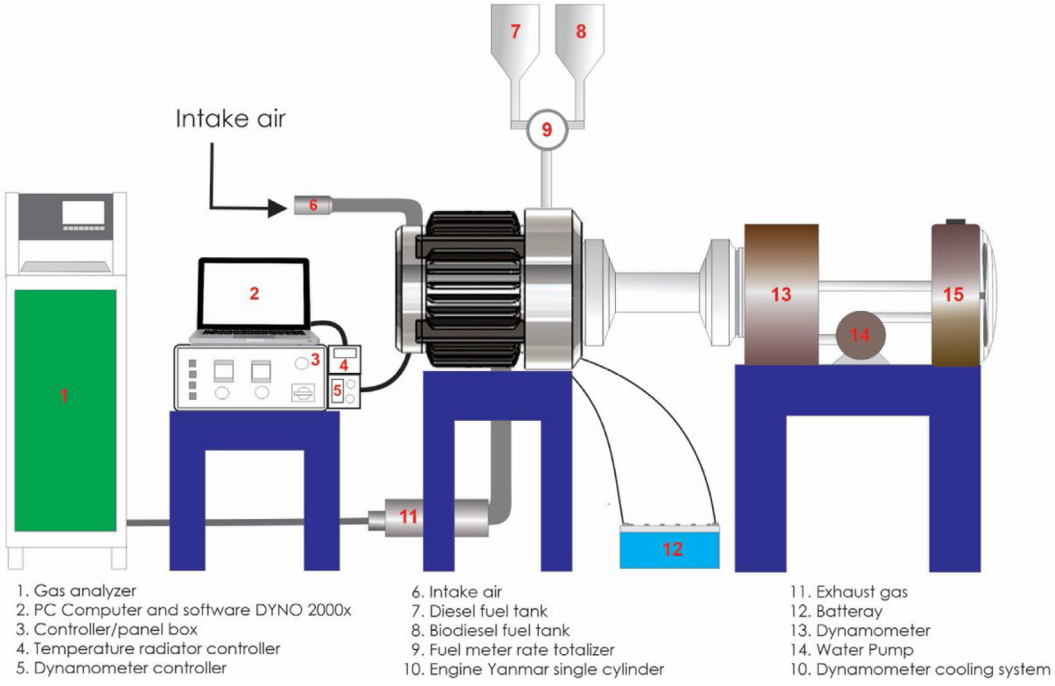

Fig. 1. Schematic layout of the direct injection diesel engine experimental setup.

The ANN architecture consists of three layers named input, hidden and output layers, connected through the neurons. The back-propagation with Levenberg–Marquard was used in this study. For all the ANN models, the engine's speed and fuel type were considered the input function to predict the BSFC, BTE and emissions. The ANN was trained until the minimum Mean Square Error (MSE) was reached and the average Correlation Coefficient (R) was closed or equal to 1.

2.7. ELM Modelling

Extreme Learning Machine (ELM) was initially developed for single-hidden-layer feed-forward networks (SLFNs). Single-hidden layer feed-forward neural networks (SLFN) are widely used to approximate complex nonlinear mappings directly from the input samples where the hidden layer parameters in the ELM are initialised randomly. The output weights were calculated using Moore–Penrose generalised inverse. The output function of the ELM for generalised SLFNs (Eq. (4)) is given by (Wong et al., 2013; Wu et al., 2013):

$$f_L(x) = \sum_{i=1}^{L} \beta_i G(w_i, b_i, x), \quad x \in R^n, a_i \in R^n \tag{4}$$

where w_i and b_i are the hidden notes learning parameters. β_i is the weight which connects the ith hidden note and the output node. $G(wa_i, b_i, x)$ shows the output value of the ith hidden note for the input x. The additive hidden note with the activation function of $g(x) : R \to R$ (e.g., sigmoid and threshold), $G(w_i, b_i, x)$ (Eq. (5)) is:

$$G(w_i, b_i, x) = g\left(\sum_{j=i}^{n} w_{ij} x_j + b_i\right), \qquad b_i \in R \tag{5}$$

where $w_{ij} = [w_{i1}, w_{i2}, \ldots, w_{in}]^T$ is the weight vector which connects the input layer and ith is the hidden node to i with input to j. Also, b_i is the bias of the ith the hidden node a_i, $x = [x_1, x_2, \ldots, x_n]^T$ is the inner product of vector a_i in R^n.

Using Eq. (3) can find G (w_{ij}, b_i, X) for RBF hidden note with activation function $g(x) : R \to R$ (e.g., Gaussian) (Eq. (6)) :

$$G(w_i, b_i, x) = g\left(b_i \sqrt{\sum_{j=i}^{n} (x_j - w_{ij})^2}\right)^T, \quad b \in R^+ \tag{6}$$

w_i and b_i represent the center and impact factor of ith RBF node, R^+ represent set of all positive real values. A particular case of SLFN that has RBF nodes in its hidden layer forms RBF network. For N, arbitrary distinct samples $(x_i, t_i) \in R^n x R^m$ where, n x 1 input vector is represented by x_i and m x 1 target vector is represented by ti. If an SLFN with L hidden nodes approximates N samples with zero error then it implies there exist β_i, w_i and b_i such that.

$$f_i(x) = \sum_{i=1}^{L} \beta_i G(w_i, b_i, x), \; j = 1, \ldots, N \tag{7}$$

Eq. (7) may expressed compactly as

$$H\beta = T \tag{8}$$

where

$$H\left(\tilde{w}, \tilde{b}, \tilde{x}\right) = \begin{bmatrix} G(w_1, b_1, x_1) & \ldots & G(w_L, b_L, x_1) \\ G(w_1, b_1, x_N) & \ldots & G(w_L, b_L, x_N) \end{bmatrix}_{NxL} \tag{9}$$

With $\overline{w} = w_1, \ldots, w_L; \tilde{b} = b_1, \ldots, b_L; \tilde{x} = x_1, \ldots, x_L$

$$\beta = \begin{bmatrix} \beta_1^T \\ \vdots \\ \beta_L^T \end{bmatrix}_{Lxm} \quad and \; T = \begin{bmatrix} t_1^T \\ \vdots \\ t_L^T \end{bmatrix}_{Nxm} \tag{10}$$

H is the hidden layer output matrix of SLFN with ith column of H being the ith hidden node's output with respect to inputs x_1, …, x_n (Eqs. (8)–(10)).

Unlike traditional learning algorithms, the ELM tends to reach the slightest training error and the smallest norm of output weights compared to the conventional learning algorithms, making the regression performance better. The essence of ELM is

that the hidden layer parameters can be independent of training samples, and the hidden layer of the generalised SLFNs need not be tuned (Wong et al., 2015a; Wu et al., 2013).

2.8. Random subsampling cross-validation of ELM

Therefore random sub-sampling validation cross-validation was adopted in this study to evaluate the performance of the modelling methods for ELM (Wong et al., 2013; Yuan, 2015). Random sub-sampling is multiple holdouts based on randomly splitting the data into subsets, whereby the user defines the size of the subsets. We used 48 data for training and 12 data for testing and repeated 10 times.

2.9. Data verification for ANN and ELM

The coefficient of determination (R^2), and mean absolute percentage error (MAPE), which as defined below was used to determine the performance of the both mathematical modellings (Eqs. (11)–(12)):

$$R^2 = 1 - \sum_{i=1}^{n} \left(\frac{(y_{ei} - y_{pi})^2}{(y_m - y_{pi})^2} \right) \tag{11}$$

$$MAPE = \sum_{i=1}^{n} \left| \frac{y_{ei} - y_{pi}}{y_{ei}} \right| \times 100\% \tag{12}$$

where n is the number of experimental data while y_{ei} is the experimental output value, y_{pi} is the predicted output value and y_m is the average experimental output value. The greatest R^2 and the smaller MAPE were acquired to define the accuracy and performance of the mathematical model.

3. Results

3.1. Properties biodiesel diesel blends

Table 3 measures and tabulates the physicochemical properties of diesel, biodiesel, and blended biodiesel–diesel fuels. SFME's overall fuel characteristics were satisfactory. However, they had a slightly higher viscosity (5.92 mm^2/s) and a lower calorific value (40.493 MJ/kg) as compared to diesel (2.91 mm^2/s and 45.83 MJ/kg). Furthermore, SFME's oxidation stability was 4.42 h, which is less than the EN 14214 requirement of 6 h. On the other hand, SFME achieved more oxidative stability than the ASTM D6751 recommended limit of 3.0 h (minimum value). Blending SFME with diesel fuel has improved the overall oxidation stability of the blended fuel (10–16.5 h), which are a highly recommended method to improve the target properties. The presence of cyclopropene ester in SFME's malvalic (2.19%) and sterculic acids (45.12%) causes oxidation stability to be reduced. The cyclopropene ring have a weaker carbon chain than palmitic (22.75%), oleic (7.71%), (linoleic (11.70%), steric (6.04%), and arachidic acid (2.96%) of carbon chains. Other fatty acid methyl ester such as lauric (0.13%), myristic (0.26%), palmitoleic (0.26%), and linolenic acid (0.90%) was found less than 1%. Due to high value of cyclopropane ester, thus SFME is susceptible to fast oxidation. The flash point of SFME is higher than that of diesel by 85 °C. Hence, when the biodiesel concentration in blends increased, the blended fuel's kinematic viscosity, density, and flash point rose due to the function of biodiesel's properties. However, biodiesel's calorific value is much lower than diesel by 5.34 MJ/kg. Hence we expected that the calorific value of the blending fuel will decreases as the concentration of biodiesel increases, as shown Table 3. Additionally, the increased flash point property revealed that biodiesel is safer to store and use in transportation sector. Low oxidation stability was the limitation of SFME, but blending with diesel, improved the stability of the blended fuel. Hence SFME and diesel fuel are ideal fuels that work to compromise each shortage and benefits in terms of fuel property.

3.2. Engine performance and exhaust emissions

3.2.1. Brake thermal efficiency (BTE)

The experiment was conducted using diesel and *Sterculia foetida* biodiesel fuel blends (SFB5, SFB10, SFB20 and SFB30) in a diesel engine. The performance and emission characteristics of biodiesel–diesel blends and diesel are examined and discussed. As demonstrated in Fig. 2, the BTE trend for SFB5 is slightly higher than diesel but still comparable. SFB10 till SFB30 had lower BTE than SFB5 and diesel, indicating that SFB5 and diesel have better combustion properties and lower viscosity than other blends. SFB5 was shown to be more appropriate than other blends with greater BTE values. At 1900 rpm, the maximum BTE for SFB5, SFB10, SFB20 and SFB30 were 25.96%, 21.28%, 20.25% and 19.28%, respectively. The SFB's increased the viscosity that caused poorly formed fuel sprays, which affected the engine's combustion (Misra and Murthy, 2011). Increased viscosity causing poor spray atomisation and formed bigger droplets that significantly interrupt the complete combustion. Other than that, another element determining the BTE is the calorific value of the biodiesel. Furthermore, it is seen that when engine speed reaches a specific limit, the thermal efficiency trend reverses and begins to decrease as a function of fuel blends concentration, which is consistent with the findings of Vairamuthu et al. (2016). Moreover, better mixture formation of 5% of *Sterculia foetida* biodiesel and diesel fuel with air is the result of better air utilisation.

3.2.2. Brake specific fuel consumption (BSFC)

Fig. 3 depicts the BSFC trend of *Sterculia foetida* biodiesel–diesel blend and diesel operation at various engine speeds. At 1900 rpm, the optimum BSFC for SFB5, SFB10, SFB20, and SFB30 were approximately −5.86%, 26.87%, 30.91% and 38.79% than diesel fuel, respectively. While at 2400 rpm, the highest BSFC values were obtained, diesel, SFB5, SFB10, SFB20, and SFB30 were approximately 681, 603, 869, 907, and 951 g/kWh. SFB10–SFB30 blends shown higher fuel consumption than diesel and SFB5, which caused by fuel's properties such as higher density and viscosity. The average 22% increment in BSFC is observed in comparison with neat diesel. Generally, the BSFC will decrease when the engine speed's increases. Indeed, the decreases in BFSC were found when the engine speed is increased from 1300 to 1900 rpm, followed by a slight increase after the engine speed exceeds 1900 rpm. BSFC increases with an increase in biodiesel concentration in the blends. This result is consistent with the result found by Qi et al. (2009) that engines required more amount of biodiesel in order to obtain similar BSFC of diesel fuel. Hence, SFB30 required the highest BSFC among all tested fuel blends. The result was due to the low calorific value of the biodiesel. In this study, the difference between diesel and SFME was 5.34 MJ/kg. Engine fuel with SFB10 and above will produce lower brake torque due to the low energy content of biodiesel blends. A similar finding was found in Buyukkaya (2010) and Hebbal et al. (2006), both of them noted that the fuel consumption for a higher percentage of biodiesel in the blends is larger to produce the same amount of energy.

3.2.3. Nitrogen oxides (NO_X)

Fig. 4 illustrates the NO_x (ppm) emissions at full throttle at engine speed varies from 1300 rpm to 2400 rpm for SFB with diesel as the baseline. The NO_x emissions for SFB5, SFB10, SFB20 and SFB30 were higher than diesel fuel by 17.49%, 26.67%, 31.78%,

Table 3
Properties of petrol diesel, biodiesel and biodiesel diesel blends.

Properties	Unit	Range values	Standard method	Diesel	SFME	SFB5	SFB10	SFB20	SFB30	SFME (Kavitha and Murugavelh, 2019)
Kinematic viscosity at 40 °C	mm^2/s	1.9–6.0	ASTM D445	2.91	5.92	3.24	3.6	4.05	4.6	5.67
Density at 15 °C	kg/m^3	860–900	EN ISO 3675	839	876.9	822.6	841.5	848.5	857.8	932
Acid value	mg KOH/g	0.5 (max.)	ASTM D664	0.17	0.38	0.17	0.17	0.18	0.18	0.74
Calorific value	MJ/kg	–	EN 14214	45.83	40.49	45.32	45.25	44.15	43.86	38.39
Flash point	°C	100–170	ASTM D93	71.5	156.5	80.5	82.5	85.5	87.5	162
Pour point	°C	−15–16	ASTM D97	1	2.8	1	2	3	3	−3
Oxidation stability at 110 °C	h	3 (min.)	EN 14112	23.7	4.42	16.45	15.34	11.39	10.2	–

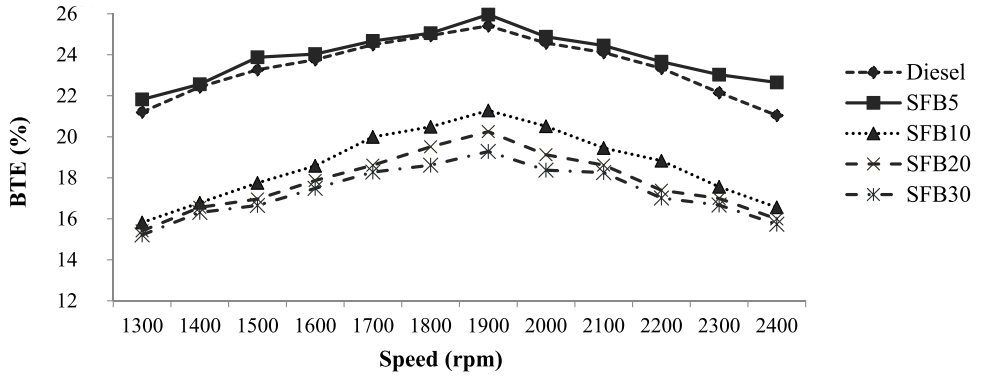

Fig. 2. BTE with various engine speeds at full throttle for blended fuels and diesel.

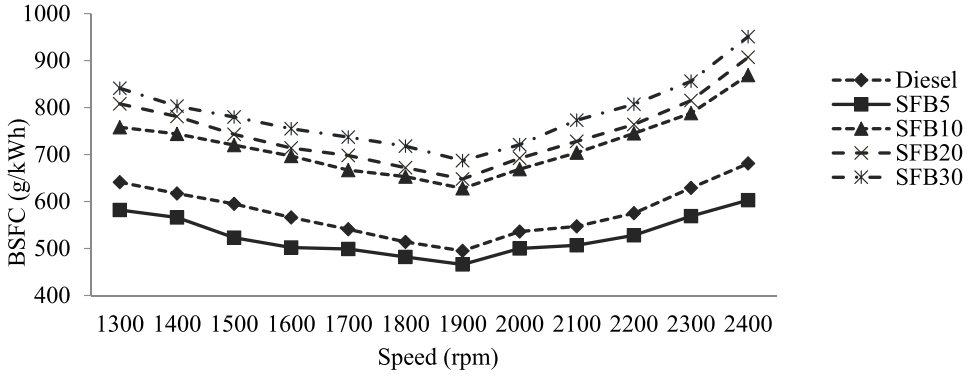

Fig. 3. BSFC with engine speed vary at 1300 to 2400 rpm at full throttle for the blended fuels and diesel.

and 37.50%, respectively, when compare with baseline diesel fuel. It is evident that all of the *sterculia foetida* biodiesel diesel blends have significantly higher NO_x emissions than diesel. The highest amount of NO_x emissions was found at an engine speed of 2400 rpm for all fuel blend. Injection timing and injection pressure was one of factor affecting the combustion temperature that eventually influenced the NO_x emissions. This study shows that higher engine speed and higher concentration of *sterculia foetida* biodiesel in the blend will cause higher NO_x emissions. Higher NOx emissions are due to higher oxygen content percentages in the blended fuel that caused higher combustion temperature in the premixed and diffusion combustion phase. At lower engine speed, the NO_x emissions for SFB5, SFB10, SFB20 and SFB30 are higher than diesel fuel with a value of 222.4, 238.6, 250.1, and 261.1 ppm vol., respectively. The NO_x emissions is 152 ppm vol. for diesel fuel. The NO_x emissions is lesser during low engine speed is due to weak air swirl movement and low in-cylinder heat temperature. Besides, the biodiesel's cetane number will also deliver more NO_x emissions during high engine speed (Misra and Murthy, 2011; Çelikten et al., 2012). Then, high cylinder temperature and exhaust temperature means there is an increase in the efficiency of combustion and the performance efficiency of the engine. Similar finding can be obtained from Karabektas et al. (2008) and Nabi et al. (2009). The higher engine's air/fuel ratio and higher peak pressure of blended fuel also lead to higher NO_x emissions. The presence of oxygen in the blends cause an increase in the combustion temperature that cause higher NO_x formation, indicating high exhaust temperature (Lin et al., 2009). According to Keskin et al. (2008), increasing biodiesel concentration in the biodiesel–diesel blend causes a small rise in NO_x emissions. However, the NOx emissions depend on various parameters, such as biodiesel type, engine technology, operation conditions, combustion temperature, and injection parameter.

3.2.4. Carbon monoxide (CO)

Fig. 5 shows the trend of CO emissions for SFB blended fuel and compare with the diesel as baseline. CO emissions for SFB blended fuel were less than diesel for all varied engine speed. At 1900 rpm, the CO emissions for SFB5, SFB10, SFB20 and SFB30 were lower than diesel fuel by 8.73%, 18.86%, 26.77%, and 35.58%, respectively. Besides, higher speed (2400 rpm) produces lesser CO emission than low engine speed (1300 rpm). CO emissions decreases especially during high engine speed due to turbulence occurs in the combustion chamber. According to Ilkılıç and Aydın

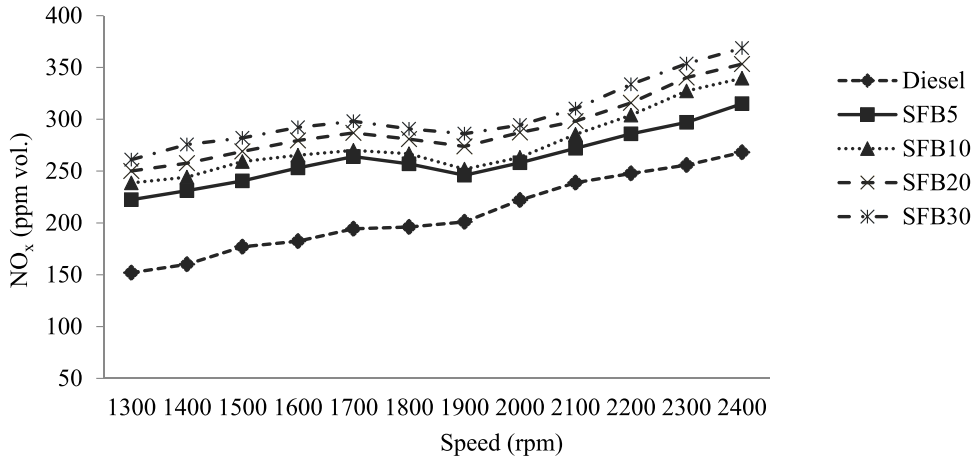

Fig. 4. NO_x emissions with varied engine speed for the blended fuels and diesel.

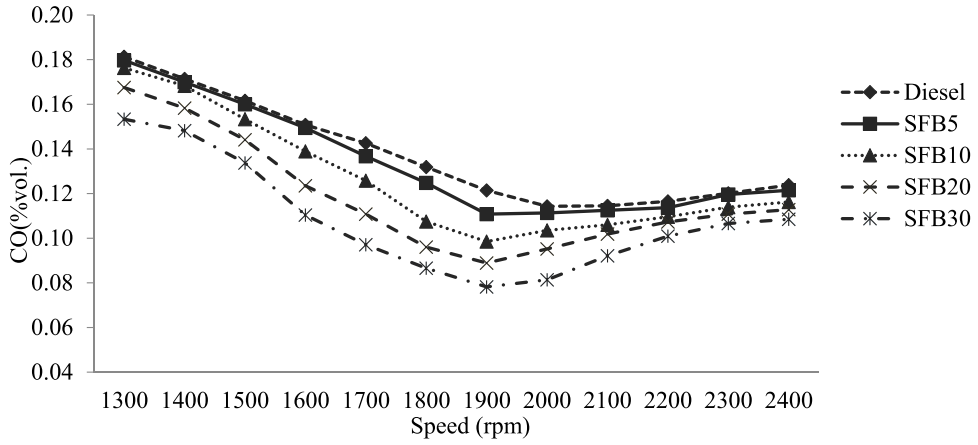

Fig. 5. CO emissions with varied engine speed for the blended fuels and diesel.

(2011) and Muralidharan et al. (2011) finding, the rising temperature in the combustion chamber cause incomplete combustion in the chamber that cause CO emission increases. Significant reduction in CO can be observed at 1900 rpm for SFB30 in comparison with diesel. At higher engine speed, the difference of CO emission for blended fuel with diesel fuel was less than 0.02%. SFB5 have similar CO emission compared with diesel fuel. Fuel viscosity will affect the fuel spray quality, which will cause increases in CO emission. However, it is not the same cause for this study. The blended fuel with *sterculia foetida* biodiesel showed marginal reduction in CO emission and it was due to improvement in the combustion that caused by the presence of biodiesel. Biodiesel has higher cetane number which will helps to shorter the ignition delays and reduces the CO emission especially at higher speed diesel engines. Moreover, it is apparent that a higher concentration of biodiesel in the blend will cause lesser CO emissions in this study. It may be due to limited time for a combustion cycle, which causes less formation of CO. It produced more unburned hydrocarbon, as shown in Fig. 7. Preheating the biodiesel blends might be one method to improve the performance of the combustion chamber in the engine, which contributes to improving the quality and efficiency of the combustion. That will reduce the CO and HC emissions in the exhaust. Besides, inlet air temperature is one of the factors that will also influence CO emission. The high air temperature will cause a higher in-cylinder temperature that will encourage the occurrence of oxygen with *sterculia foetida* biodiesel.

3.2.5. Carbon dioxide (CO_2)

Fig. 6 illustrates the CO_2 emissions for SFB at various speeds compared with diesel fuel. Complete combustion can be seen for SFB5 blends as it emits more CO_2 emission than the other blend, including diesel fuels. The CO_2 emission for SFB5 is more 3.01% than diesel fuel, whereas the CO_2 emission of SFB10, SFB20, and SFB30 were 1.63%, 5.78%, and 9.57%, respectively, lesser than diesel fuel. The result shows that SFB5 has higher CO_2 emissions than diesel fuel. It is generally known that adding biodiesel with diesel will reduce the CO_2 emission, but it is not for SFB5. Hence SFB is much superior to diesel and other blending ratios. The oxygen content in the biodiesel will cause more carbon to be oxidised into CO_2. Fig. 6 shows that a higher concentration of biodiesel (SFB10, SFB20 and SFB30) in the fuel blend will lower the CO_2 emission than diesel fuel (2.95%). The maximum difference between diesel and SFB30 is approximately an 8.52% reduction in CO_2 emission. A higher concentration of *sterculia foetida* biodiesel reduces CO_2 emission. One of the reasons for causing a reduction in CO_2 emission was the viscosity of the blended fuel. The viscosity of the blended fuel is increases as the concentration of biodiesel increases. The effect of biodiesel viscosity will interfere fuel consumption. Higher viscosity will reduce the size of the droplet done by spray atomisation. Atomisation will ensures complete evaporation of liquid fuel and prepares for a combustible mixture for combustion. A bigger droplet will cause incomplete combustion and reduce the CO_2 emission while causing the formation of CO and unburned hydrocarbon. Besides, the lower calorific value of the biodiesel blends will cause higher fuel

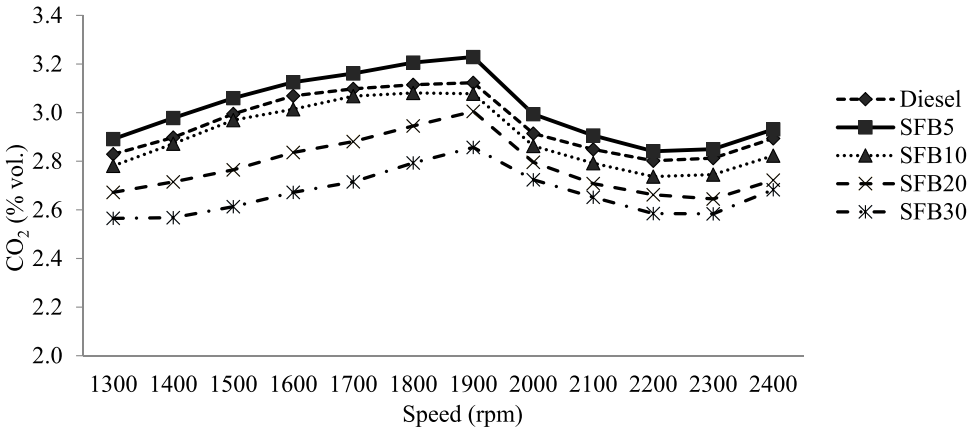

Fig. 6. CO_2 emissions with varied engine speed for the blended fuels and diesel.

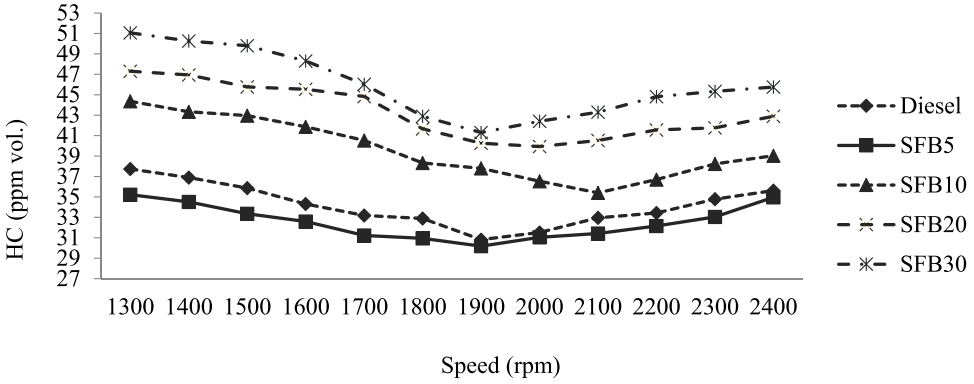

Fig. 7. HC emissions with varied engine speed for the blended fuels and diesel.

consumption, where extra fuel was needed to produce the same engine power.

3.2.6. Hydrocarbon (HC)

The HC emission values of *sterculia foetida* biodiesel–diesel blends and diesel fuel within an engine speed of 1300–2400 rpm are shown in Fig. 7. It is apparent that the HC emission is highest for SFB30 compared with other blend mixtures and diesel fuel at 1300 rpm. At low speed, HC emission for diesel, SFB5, SFB10, SFB20, and SFB30 was 37.73, 35.22, 44.36, 47.3 and 51.1 ppm vol., respectively. The lowest HC emission was found at engine speed set at 1900 rpm. The diesel, SFB5, SFB10, SFB20, and SFB30 was 30.82, 30.18, 37.8, 40.26 and 41.3 ppm vol. It can be observed that the HC emission is lowest for SFB5 when compared with that for diesel fuel. SFB5 was superior in helping to reduce the HC emission compared with diesel fuel. It can be clarified that the biodiesel fuel's oxygen content will enhance the combustion process and reduce the unburned hydrocarbon. However, for a higher concentration of biodiesel, the HC was higher than diesel fuel. The reason might arise from an increment in other physiochemical properties such as viscosity, density, and calorific value after the blending.

3.2.7. Smoke opacity

Fig. 8 shows the smoke opacity with an engine speed range of 1300–2400 rpm for the SFB blended fuels and diesel. Smoke opacity indicates the amount of dry soot and emission of particulate matter. The oxidised carbon that forms at the reaction zone is called soot oxidation. The soot will be produced when the oxygen or local temperature does not support the oxidation process. It is evident that the SFB5 possesses better combustion characteristics that induce complete combustion. For example, an engine speed of 1900 rpm shows optimal combustion as it produces the lowest smoke opacity. The SFB5 produced the lowest smoke opacity with a value of 14.46% HSU, while diesel fuel produced smoke opacity of 14.92% HSU. There is a significant reduction in the smoke opacity by adding 5% of *sterculia foetida* biodiesel into diesel fuel. The results show that SFB5 indicates better emission performance when compared with diesel fuel. Other blended fuels show incomplete combustion indicated by lower thermal efficiency and higher smoke opacity, where SFB10, SFB20 and SFB30 produce smoke opacity with a value of 15.15%, 20.44% and 21.12% HSU, respectively. The smoke opacity is marginally higher for a high concentration of *sterculia foetida* biodiesel in the fuel blends due to the viscosity and volatility of biodiesel. In addition, it causes a larger fuel droplet size and reduces the fuel/air mixing rate, resulting in poor spray formation in the combustion chamber. A significant difference in smoke opacity between the test fuels was found on high engine speed (2400 rpm). As mentioned above, diesel and low *sterculia foetida* biodiesel fuel blends have better combustion characteristics. It might be due to the presence of oxygen molecules in the methyl ester that encourages complete combustion during rich diffusion. This outcome was similar to Senthil Kumar and Jaikumar (2014) and Haldar et al. (2009) found that increasing the biodiesel ratio in the blends resulted in slightly higher smoke opacity emission than diesel.

3.3. ANN and ELM modelling performance evaluation

All of the modelling methods were written in MATLAB R2012a and run on a PC with an Intel Core i7 processor and 8 GB of

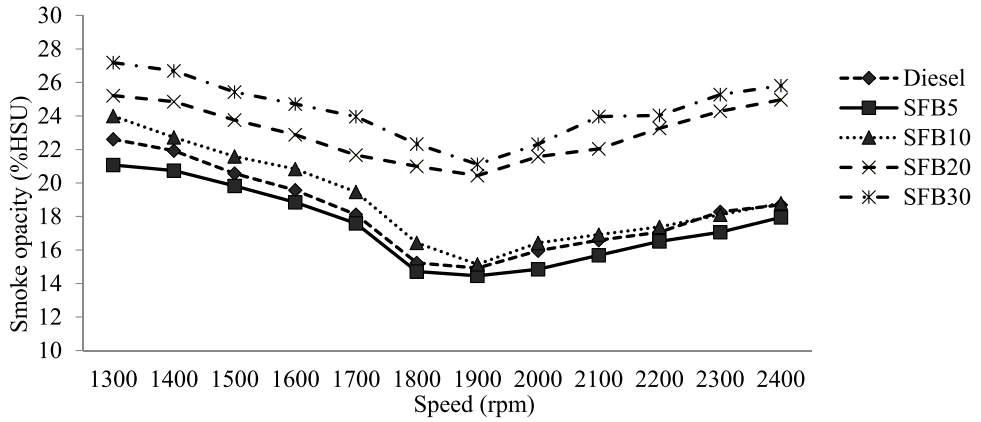

Fig. 8. Smoke opacity produced from varied engine speed for blended fuels and diesel.

Table 4
Random subsampling cross-validation.

	Output variable	Average MAPE
Performance	BSFC	0.7009
	BTE	1.0497
Emission	CO	0.4471
	CO_2	0.2609
	NO_x	0.4056
	Smoke opacity	0.5666

RAM running Windows 8. The reports of the subsampling cross-validation were combined and averaged to show how accurately the models could perform Table 4. The statistical analysis for the performance and emission model revealed that the developed ELM model had low MAPE than ANN (Table 5). The MAPE for ANN model for BSFC and BTE were 1.4687 and 1.8148, respectively while the coefficient of determination (R^2) were 0.9906 and 0.9808, respectively. Meanwhile, the MAPE for the ELM model for BSFC and BTE were 0.4101 and 0.7929, respectively, while the R^2 were 0.9961 and 0.9879, higher than ANN model. Both mathematical models were used to predict the emission, and Table 6 shows predicted results. Hence, ELM are better than ANN by 0.55% for BSFC and 0.71% for BTE.

Based on ANN prediction, the MAPE for CO, CO_2, NO_x, HC and smoke opacity were 1.5124, 0.5618, 1.6427, 0.2549, and 1.5363, respectively. Their R^2 were 0.993, 0.985, 0.984, 0.977 and 0.987, respectively. The developed ANN model can preciously predict the fuel emission (>97%). Furthermore, the ELM model able to predict the fuel emission even more accurately than ANN model (>98%). The MAPE of ELM model for CO, CO_2, NO_x, HC and smoke opacity were 0.2137, 0.1925, 0.3102, 0.1325, and 0.3565, respectively, while the R^2 were 0.999, 0.991, 0.998, 0.988 and 0.995, respectively. The differences in R^2 for ANN and ELM for CO, CO_2, NO_x, HC and smoke opacity were 0.6%, 0.6%, 1.4%, 1.1% and 0.8%, respectively. The difference indicated that ELM is superior than ANN in predicting pollutant produced by SFME. The R^2 value for all the data was close to 1 and it indicates that there is a strong correlation in modelling of both performance and emission.

3.4. Performance comparison of ANN and ELM

Based on the MAPE and R^2 for both ANN and ELM modelling, ELM shown superior prediction model when compare with ANN. Fig. 9 showed the prediction accuracy and error statistical indicator result for the both ANN and ELM models. ELM model able to accurately predict the engine performance and fuel emission with relatively minimal error than ANN model. The analytical method adopted by ELM model was to solve based on the output weights by single step. Whereby, ANN used the iterative method to calculate the support vectors which make the accumulative error resulting from all the steps may become large when the final solution is returned. Therefore, ELM has a smaller error compared than ANN. Small error means ELM is a more suitable prediction model for this study.

4. Conclusion and future recommendation

Sterculia foetida biodiesel is a promising non-edible feedstock that can be used in conjunction with diesel fuel in an engine. This study has explored the engine performance and exhaust emission characteristics of blended *sterculia foetida* biodiesel with diesel, employing experimentation, ANN and ELM modelling. The conclusion of this study are as below:

- Blending of SFME with diesel fuel enhances the blended properties, especially viscosity and flash points. The blended fuels in this study met the specification stipulated in the D6751 or EN 14214 standard. The oxidation stability of the blended fuels meets the minimum requirement of the standard methods, with a value of more than 10 h.
- Among the blended fuel, SFB5 was seen as the promising blending ratio among the blended fuel as it delivers better engine performances (decreasing BSFC, increasing BTE) compared with diesel fuel. Besides, SFB5 shows better exhaust emissions compared to diesel fuel. SFB10, SFB20, and SF30 caused a marginal increment in NO_x, HC and smoke opacity except CO and CO_2.
- A comparison between ELM and ANN modelling under the same sample data sets was conducted in this study. The MAPE and R^2 results comparison show that the ELM modelling is superior to ANN. Therefore, it can be concluded that ELM is a promising technique for engine performance and emission exhaust application.

In short, the proposed comparison modelling predictions for the engine performance and exhaust emissions resulted in a better performance than ANN modelling. Based on the study, SFB5 is the most favourable blend that can outperform diesel fuel and it verified that *sterculia foetida* biodiesel was a great asset to the biofuel industry. Moreover, this study deduced that the ELM modelling has excellent generalisation capability to precisely predict the engine performance and important emission parameters for different blending fuels and other biodiesel feedstocks. Besides, this study's experimental and numerical work will provide an overview to researchers, scientists, and the automotive industry to develop a new approach or modelling based on our study.

Table 5
Experimental design matrix and experiment result for engine performance.

Run	Speed (rpm)	Fuel	Performance					
			BSFC			BTE		
			Experiment	ANN prediction	ELM prediction	Experiment	ANN prediction	ELM prediction
1	1300	Diesel	641	629.31	640.93	21.84	21.58	21.83
2	1400		617	609.06	598.17	21.05	22.45	21.07
3	1500		595	586.09	583.86	23.03	23.85	23.03
4	1600		566	562.23	565.96	26.33	25.79	26.35
5	1700		541	540.10	533.54	28.25	28.12	28.24
6	1800		514	523.19	513.94	24.38	24.42	25.71
7	1900		495	515.58	495.06	24.27	22.62	24.28
8	2000		536	521.11	535.91	24.21	23.82	24.21
9	2100		547	541.76	547.02	23.47	23.64	23.47
10	2200		575	575.98	580.73	22.57	23.02	23.30
11	2300		629	618.21	639.97	25.13	23.27	25.12
12	2400		681	660.68	680.9	25.49	25.05	25.50
13	1300	SFB5	582	585.05	582.08	28.09	28.27	28.10
14	1400		566	562.00	566.00	31.60	31.55	33.52
15	1500		523	537.85	523.09	37.04	34.70	37.03
16	1600		502	513.4	502.02	30.68	30.51	30.69
17	1700		499	490.6	499.04	31.14	30.97	31.14
18	1800		482	472.92	486.92	30.64	32.48	30.91
19	1900		466	464.83	466.10	31.27	32.01	28.79
20	2000		500	470.58	491.55	30.80	29.76	30.79
21	2100		507	492.53	506.99	27.75	27.43	27.75
22	2200		528	529.44	528.06	26.52	26.76	26.52
23	2300		569	575.81	569.03	28.39	28.74	28.39
24	2400		603	623.61	603.12	32.43	32.39	32.42
25	1300	SFB10	758	768.93	757.96	39.04	38.98	39.03
26	1400		744	741.65	743.97	31.50	31.64	31.51
27	1500		720	713.51	718.86	31.88	31.85	30.54
28	1600		697	686.92	696.94	32.89	32.94	32.89
29	1700		667	665.13	657.61	32.46	33.02	32.46
30	1800		653	651.82	652.94	31.89	31.37	31.88
31	1900		628	650.54	628.00	20.80	21.25	20.81
32	2000		669	664.16	626.23	19.29	18.66	19.29
33	2100		704	694.13	703.95	20.75	18.90	20.75
34	2200		745	739.09	744.94	21.90	21.79	21.9
35	2300		788	793.83	788.08	24.31	24.34	24.31
36	2400		869	850.37	868.86	22.08	21.98	22.09
37	1300	SFB20	808	815.41	808.00	22.40	21.85	22.4
38	1400		781	778.59	781.03	22.34	22.75	22.34
39	1500		743	742.67	752.82	23.06	22.80	23.06
40	1600		714	710.15	714.02	22.62	21.35	22.61
41	1700		698	684.05	698.01	19.03	19.05	19.04
42	1800		672	667.83	671.97	18.62	18.39	18.62
43	1900		648	665.15	648.09	19.86	19.78	18.81
44	2000		692	679.42	691.96	20.97	20.99	20.97
45	2100		728	712.58	727.99	22.46	22.38	22.46
46	2200		764	763.64	763.97	21.40	21.67	21.40
47	2300		815	827.67	815.14	21.45	21.22	21.45
48	2400		907	896.68	906.96	21.27	21.05	19.68
49	1300	SFB30	841	844.96	840.94	22.04	22.12	22.04
50	1400		803	806.92	803.07	21.91	21.75	21.91
51	1500		780	771.92	779.96	18.07	18.28	18.07
52	1600		755	742.16	755.00	18.01	17.72	18.01
53	1700		737	720.03	737.00	19.10	19.38	19.1
54	1800		718	708.14	718.00	20.76	20.58	20.76
55	1900		687	709.35	709.08	22.26	21.12	22.26
56	2000		721	726.38	720.99	21.19	21.36	21.19
57	2100		773	761.01	772.98	21.49	21.48	21.31
58	2200		807	812.56	806.99	21.16	21.54	20.70
59	2300		856	876.57	856.10	21.51	21.45	20.84
60	2400		951	945.18	950.89	20.84	20.97	20.84
MAPE				1.4687	0.4101		1.8148	0.7929
R^2				0.9906	0.9961		0.9808	0.9879

ELM modelling is beneficial for biodiesel research, and it can be applied to various types of biodiesel and biodiesel blends. Moreover, our study found that all *sterculia foetida* biodiesel–diesel blends investigated qualify as an alternative fuel in diesel engines. SFB5 was superior among the blended fuel and even performed much better than diesel as an emission reduction fuel.

Preheating the biodiesel–diesel blend before the blends were introduced into the diesel engine and varied inlet air temperature

Table 6
Experimental design matrix and experiment result for engine emission.

Run	Speed (rpm)	Fuel	Emission														
			CO			CO_2			NO_x			HC			Smoke opacity		
			Experiment	Prediction		Experiment	Prediction		Experiment	Prediction		Experiment	Prediction		Experiment	Prediction	
				ANN	ELM		ANN	ELM		ANN	ELM		ANN	ELM		ANN	ELM
1	1300	Diesel	0.181	0.185	0.181	2.83	2.83	2.83	152	160.11	152.01	37.73	35.544	37.73	22.61	21.99	20.83
2	1400		0.171	0.174	0.171	2.9	2.91	2.9	160	165.08	163.16	36.9	36.903	36.98	21.93	21.36	21.92
3	1500		0.162	0.163	0.162	3	2.99	2.99	177	177.63	176.99	35.86	35.211	33.86	20.57	20.48	20.57
4	1600		0.151	0.153	0.151	3.07	3.05	3.07	182.3	189.8	182.31	34.31	32.282	34.31	19.57	19.32	19.57
5	1700		0.143	0.142	0.143	3.1	3.1	3.1	194.4	194.5	195.34	33.18	35.179	33.18	18.11	17.87	18.11
6	1800		0.132	0.13	0.132	3.12	3.15	3.12	196	196.37	201.96	32.89	32.888	34.52	15.23	16.25	15.23
7	1900		0.121	0.121	0.121	3.12	3.12	3.12	201	200.48	209.8	30.82	30.82	30.72	14.92	15.11	14.92
8	2000		0.114	0.117	0.114	2.91	2.92	2.97	222	211.12	222	31.53	31.533	31.53	15.95	16.02	15.95
9	2100		0.115	0.118	0.114	2.85	2.83	2.85	238.9	230.34	235.09	32.96	32.963	32.85	16.58	16.72	16.58
10	2200		0.117	0.119	0.117	2.8	2.83	2.8	247.7	252.54	247.7	33.43	33.432	33.43	17.06	17.21	17.06
11	2300		0.12	0.121	0.12	2.81	2.86	2.81	255.8	268.63	255.76	34.78	36.781	34.561	18.28	18.12	17.79
12	2400		0.124	0.122	0.124	2.89	2.9	2.89	268.1	276.77	262.66	35.62	35.618	35.52	18.7	18.57	18.7
13	1300	SFB5	0.18	0.18	0.18	2.89	2.89	2.85	222.4	225.06	222.39	35.22	38.22	35.56	21.07	21.85	20.91
14	1400		0.17	0.169	0.173	2.98	2.98	2.99	231.2	230.22	231.2	34.51	34.509	34.513	20.74	21.12	20.74
15	1500		0.16	0.158	0.16	3.06	3.06	3.06	240.5	242.03	242.67	33.36	33.358	33.46	19.83	20.13	19.83
16	1600		0.149	0.147	0.149	3.13	3.13	3.12	253	251.06	253	32.59	30.588	32.77	18.84	18.85	19.04
17	1700		0.137	0.134	0.138	3.16	3.19	3.16	264	252.17	263.99	31.23	31.7	31.231	17.59	17.29	17.58
18	1800		0.125	0.12	0.125	3.21	3.23	3.21	257	250.5	256.99	30.95	30.945	31.55	14.71	15.57	14.72
19	1900		0.111	0.111	0.111	3.23	3.21	3.23	246	250.69	246.02	30.18	28.18	30.58	14.46	14.34	14.46
20	2000		0.111	0.109	0.111	2.99	3	2.99	258	256.82	257.99	31.05	31.048	31.35	14.85	15.14	14.85
21	2100		0.113	0.112	0.114	2.91	2.89	2.87	272	271.54	272	31.42	30.419	31.421	15.69	15.78	15.53
22	2200		0.114	0.115	0.116	2.84	2.89	2.84	286	290.4	285.99	32.16	32.64	31.52	16.51	16.12	16.51
23	2300		0.12	0.117	0.12	2.85	2.9	2.89	297	304.1	297.03	33.05	33.047	33.05	17.06	17.16	17.06
24	2400		0.122	0.12	0.122	2.93	2.93	2.93	315	309.74	314.98	34.96	34.958	36.24	17.95	17.99	17.95
25	1300	SFB10	0.176	0.175	0.176	2.78	2.8	2.78	238.6	236.2	238.6	44.36	44.359	44.36	24	23.8	23.99
26	1400		0.168	0.164	0.17	2.87	2.87	2.87	244.16	243.02	244.17	43.33	43.326	43.332	22.72	22.96	22.72
27	1500		0.153	0.153	0.153	2.97	2.94	2.97	259.23	256.83	259.23	42.96	42.96	42.96	21.58	21.84	21.49
28	1600		0.139	0.141	0.139	3.01	3.01	3.01	265.3	266.26	265.31	41.86	41.862	40.36	20.84	20.41	20.84
29	1700		0.126	0.126	0.126	3.07	3.07	3.07	270.06	267.56	270.06	40.53	40.53	40.53	19.46	18.71	19.46
30	1800		0.108	0.111	0.108	3.08	3.11	3.08	266.8	265.93	266.79	38.33	38.333	37.58	16.42	16.87	16.42
31	1900		0.099	0.102	0.099	3.08	3.09	3.08	251.83	265.59	251.85	37.8	37.803	36.88	15.15	15.52	15.67
32	2000		0.104	0.102	0.103	2.86	2.89	2.94	263.26	270.46	263.26	36.53	36.528	36.559	16.43	16.19	16.39
33	2100		0.106	0.107	0.105	2.79	2.76	2.79	285.4	283.62	285.39	35.4	35.401	35.369	16.92	16.77	16.92
34	2200		0.11	0.111	0.11	2.74	2.75	2.74	303.93	301.8	303.93	36.7	36.701	36.7	17.38	16.87	17.38
35	2300		0.114	0.114	0.115	2.75	2.75	2.75	327.26	315.69	327.27	38.23	38.23	38.231	18.11	17.84	18.36
36	2400		0.116	0.117	0.116	2.82	2.78	2.82	339.6	321.3	339.59	39.03	39.031	39.53	18.79	18.94	18.79
37	1300	SFB20	0.168	0.165	0.167	2.67	2.68	2.67	250.13	248.72	250.12	47.3	47.297	46.259	25.22	25.32	25.21
38	1400		0.158	0.155	0.161	2.72	2.71	2.72	257.65	257.37	257.66	46.933	46.93	45.936	24.85	24.77	24.75
39	1500		0.144	0.143	0.144	2.77	2.76	2.76	268.98	271.15	267.69	45.766	45.765	45.726	23.75	24	23.76
40	1600		0.124	0.128	0.124	2.84	2.82	2.84	279.52	278.87	279.53	45.533	45.537	45.533	22.88	22.99	22.88
41	1700		0.111	0.11	0.111	2.88	2.89	2.88	286.9	280.7	286.88	44.833	44.832	45.833	21.66	21.82	21.66
42	1800		0.096	0.095	0.096	2.95	2.96	2.95	280.83	281.4	280.85	41.66	41.659	41.66	21	20.63	20.99
43	1900		0.089	0.09	0.089	3.01	2.98	3	273.86	283.56	280.04	40.26	40.261	40.26	20.44	19.95	20.44
44	2000		0.095	0.092	0.095	2.8	2.8	2.8	287.2	289.62	287.19	39.93	39.927	39.73	21.58	21.28	21.57
45	2100		0.102	0.099	0.102	2.71	2.68	2.71	298.2	302.65	298.2	40.53	40.527	40.33	22.03	22.65	22.04
46	2200		0.107	0.106	0.107	2.66	2.66	2.66	315.86	321.57	315.86	41.56	41.559	42.46	23.26	23.12	23.26
47	2300		0.111	0.11	0.112	2.65	2.67	2.68	340.23	337.86	340.24	41.76	41.759	39.54	24.28	24.33	24.52
48	2400		0.113	0.113	0.113	2.72	2.71	2.72	353.3	345.45	353.29	42.9	42.9	42.53	24.97	26.26	24.96
49	1300	SFB30	0.153	0.157	0.153	2.57	2.56	2.56	261.06	261.02	261.06	51.06	51.064	51.02	27.18	27.17	27.18
50	1400		0.148	0.146	0.148	2.57	2.58	2.57	275.63	272.74	275.62	50.26	50.258	51.26	26.69	26.7	26.69
51	1500		0.134	0.131	0.133	2.61	2.61	2.61	282	286.42	282.02	49.8	49.797	49.779	25.43	25.94	25.43
52	1600		0.11	0.113	0.11	2.67	2.66	2.67	292.16	292.31	292.15	48.3	48.303	48.3	24.71	24.88	24.71
53	1700		0.097	0.095	0.097	2.72	2.72	2.7	298.03	293.01	296.41	46.03	46.028	46.03	23.97	23.61	23.96
54	1800		0.087	0.084	0.087	2.79	2.79	2.79	290.83	292.58	290.83	42.9	42.897	42.9	22.32	22.31	22.32
55	1900		0.078	0.081	0.078	2.86	2.85	2.86	286.13	293.34	286.13	41.3	41.303	41.23	21.12	21.46	21.12
56	2000		0.081	0.084	0.081	2.72	2.72	2.72	294.4	298.02	294.39	42.4	42.403	42.6	22.32	22.51	22.32
57	2100		0.092	0.092	0.092	2.65	2.61	2.65	310.23	310.28	312.54	43.3	43.3	43.5	23.96	23.8	23.96
58	2200		0.101	0.101	0.1	2.59	2.62	2.59	333.76	330.84	333.76	44.81	43.51	43.807	24.03	23.87	24.03
59	2300		0.107	0.107	0.107	2.58	2.64	2.58	353.73	351.99	353.73	45.33	42.53	45.23	25.27	24.37	25.06
60	2400		0.109	0.111	0.108	2.68	2.69	2.68	368.63	364.96	368.62	45.76	45.762	45.758	25.81	25.86	25.81
MAPE				1.5124	0.2137		0.5618	0.1925		1.6427	0.3102		0.2549	0.1325		1.5363	0.3565
R^2				0.993	0.999		0.985	0.991		0.984	0.998		0.977	0.988		0.987	0.995

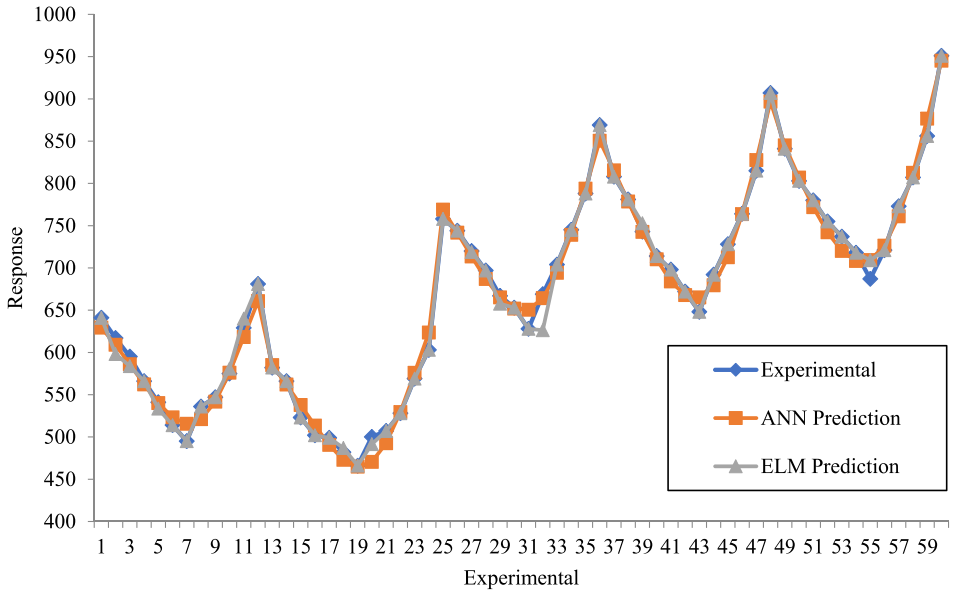

(a) BSFC

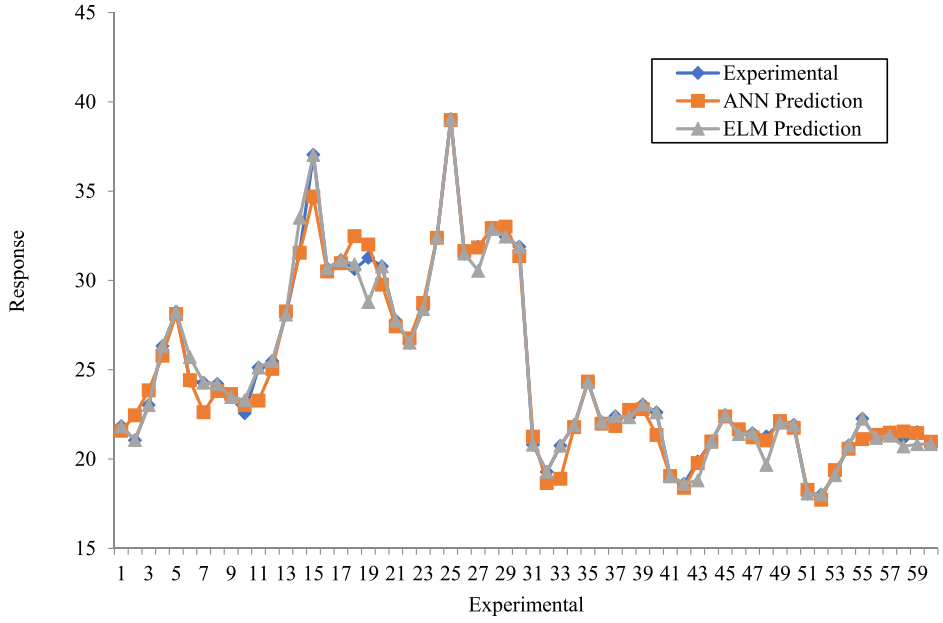

(b) BTE

Fig. 9. Comparison of engine performance experimental and predicted value.

was our limitation in this study. We hope to include these two studies in our future studies to discover the appropriate working temperature for biodiesel and the inlet air to reduce emission characteristics further. Besides, exhaust gas recirculation (EGR) can be coupled with our engine to study the function of EGR in reducing NO_x emission. We can also perform similar studies on other non-edible oil and other feedstocks available in our country or any tropical country using our prediction method and modelling. In addition, the technoeconomy of the current study can be performed to investigate the economic performance of utilising *sterculia foetida* biodiesel as one of the non-edible resources for the biodiesel industry.

Declaration of competing interest

The authors declare that they have no known competing financial interests or personal relationships that could have appeared to influence the work reported in this paper.

Acknowledgements

The authors also would like to thanks University of Technology Sydney. The authors also wish to acknowledge the financial support provided by the Direktorat Akademik Pendidikan Tinggi Vokasi Republik Indonesia, Pusat Penelitian Pengabdian Masyarakat (P3M) Politeknik Negeri Medan, Medan, Indonesia.

The authors would like to acknowledge this research as supported the AAIBE, Indonesia Chair of Renewable grant no: 201801 KETTHA at UNITEN for supporting this research.

References

Adam, I.K., et al., 2018. Performance and emission analysis of rubber seed, palm, and their combined blend in a multi-cylinder diesel engine. Energies 11 (6), 1522.

Ashok, B., Nanthagopal, K., Sakthi Vignesh, D., 2018. Calophyllum inophyllum methyl ester biodiesel blend as an alternate fuel for diesel engine applications. Alexand. Eng. J. 57 (3), 1239–1247.

Buyukkaya, E., 2010. Effects of biodiesel on a DI diesel engine performance, emission and combustion characteristics. Fuel 89 (10), 3099–3105.

Canakci, M., et al., 2009. Prediction of performance and exhaust emissions of a diesel engine fueled with biodiesel produced from waste frying palm oil. Expert Syst. Appl. 36 (5), 9268–9280.

Çelikten, İ, Mutlu, E., Solmaz, H., 2012. Variation of performance and emission characteristics of a diesel engine fueled with diesel, rapeseed oil and hazelnut oil methyl ester blends. Renew. Energ. 48, 122–126.

Chen, Z., Gryllias, K., Li, W., 2019a. Mechanical fault diagnosis using convolutional neural networks and extreme learning machine. Mech. Syst. Signal Process. 133, 106272.

Chen, X., et al., 2019b. Improvement of engine performance and emissions by biomass oil filter in diesel engine. Fuel 235, 603–609.

Dharma, S., et al., 2019. Properties and corrosion behaviors of mild steel in biodiesel-diesel blends. Energy Sources, Part A Recovery Utiliz. Environ. Effects 1–13.

Ghobadian, B., et al., 2009. Diesel engine performance and exhaust emission analysis using waste cooking biodiesel fuel with an artificial neural network. Renew. Energ. 34 (4), 976–982.

Goh, B.H.H., et al., 2020. Progress in utilisation of waste cooking oil for sustainable biodiesel and biojet fuel production. Energy Convers. Manage. 223, 113296.

Goudarzi, K., Moosaei, A., Gharaati, M., 2015. Applying artificial neural networks (ANN) to the estimation of thermal contact conductance in the exhaust valve of internal combustion engine. Appl. Therm. Eng. 87, 688–697.

Haldar, S.K., Ghosh, B.B., Nag, A., 2009. Utilization of unattended Putranjiva roxburghii non-edible oil as fuel in diesel engine. Renew. Energy 34 (1), 343–347.

Hebbal, O.D., Reddy, K.V., Rajagopal, K., 2006. Performance characteristics of a diesel engine with deccan hemp oil. Fuel 85 (14), 2187–2194.

Huang, G.-B., Zhu, Q.-Y., Siew, C.-K., 2006. Extreme learning machine: Theory and applications. Neurocomputing 70 (1–3), 489–501.

Hulwan, D.B., Joshi, S.V., 2011. Performance, emission and combustion characteristic of a multicylinder DI diesel engine running on diesel–ethanol–biodiesel blends of high ethanol content. Appl. Energ. 88 (12), 5042–5055.

Ilkılıç, C., Aydın, H., 2011. Determination of performance and exhaust emissions properties of B75 in a CI engine application. Fuel Process. Technol. 92 (9), 1790–1795.

Ilkılıç, C., et al., 2011. Biodiesel from safflower oil and its application in a diesel engine. Fuel Process Technol. 92 (3), 356–362.

Karabektas, M., Ergen, G., Hosoz, M., 2008. The effects of preheated cottonseed oil methyl ester on the performance and exhaust emissions of a diesel engine. Appl. Therm. Eng. 28 (17), 2136–2143.

Kavitha, M.S., Murugavelh, S., 2019. Optimization and transesterification of sterculia oil: Assessment of engine performance, emission and combustion analysis. J. Cleaner Prod. 234, 1192–1209.

Keskin, A., et al., 2008. Using of cotton oil soapstock biodiesel–diesel fuel blends as an alternative diesel fuel. Renew. Energy 33 (4), 553–557.

Lešnik, L., et al., 2014. Numerical and experimental study of combustion, performance and emission characteristics of a heavy-duty DI diesel engine running on diesel, biodiesel and their blends. Energ. Convers. Manage. 81, 534–546.

Lin, B.-F., Huang, J.-H., Huang, D.-Y., 2009. Experimental study of the effects of vegetable oil methyl ester on DI diesel engine performance characteristics and pollutant emissions. Fuel 88 (9), 1779–1785.

Milano, J., et al., 2021. Experimental study of the corrosiveness of ternary blends of biodiesel fuel. Front. Energy Res. 9.

Milano, J., et al., 2022. Tribological study on the biodiesel produced from waste cooking oil, waste cooking oil blend with Calophyllum inophyllum and its diesel blends on lubricant oil. Energy Rep. 8, 1578–1590.

Misra, R.D., Murthy, M.S., 2011. Performance, emission and combustion evaluation of soapnut oil–diesel blends in a compression ignition engine. Fuel 90 (7), 2514–2518.

Mofijur, M., et al., 2013. A study on the effects of promising edible and non-edible biodiesel feedstocks on engine performance and emissions production: A comparative evaluation. Renew. Sustain. Energy Rev. 23, 391–404.

Mohamed Ismail, H., et al., 2012. Artificial neural networks modelling of engine-out responses for a light-duty diesel engine fuelled with biodiesel blends. Appl. Energy 92, 769–777.

Mozaffari, A., Azad, N.L., 2014. Optimally pruned extreme learning machine with ensemble of regularization techniques and negative correlation penalty applied to automotive engine coldstart hydrocarbon emission identification. Neurocomputing 131, 143–156.

Muralidharan, K., Vasudevan, D., Sheeba, K.N., 2011. Performance, emission and combustion characteristics of biodiesel fuelled variable compression ratio engine. Energy 36 (8), 5385–5393.

Nabi, M.N., Rahman, M.M., Akhter, M.S., 2009. Biodiesel from cotton seed oil and its effect on engine performance and exhaust emissions. Appl. Therm. Eng. 29 (11–12), 2265–2270.

Oğuz, H., Sarıtas, I., Baydan, H.E., 2010. Prediction of diesel engine performance using biofuels with artificial neural network. Expert Syst. Appl. 37 (9), 6579–6586.

Qi, D.H., et al., 2009. Combustion and performance evaluation of a diesel engine fueled with biodiesel produced from soybean crude oil. Renew. Energ. 34 (12), 2706–2713.

Roy, S., Banerjee, R., Bose, P.K., 2014. Performance and exhaust emissions prediction of a CRDI assisted single cylinder diesel engine coupled with EGR using artificial neural network. Appl. Energ. 119, 330–340.

Senthil Kumar, M., Jaikumar, M., 2014. A comprehensive study on performance, emission and combustion behavior of a compression ignition engine fuelled with WCO (waste cooking oil) emulsion as fuel. J. Energy Inst. 87 (3), 263–271.

Tasdemir, S., et al., 2011. Artificial neural network and fuzzy expert system comparison for prediction of performance and emission parameters on a gasoline engine. Expert Syst. Appl. 38 (11), 13912–13923.

Tulashie, S.K., et al., 2018. Biodiesel production from shea butter: A suitable alternative fuel to premix fuel. Materialia 3, 288–294.

Vairamuthu, G., et al., 2016. Experimental investigation on the effects of cerium oxide nanoparticle on Calophyllum inophyllum (Punnai) biodiesel blended with diesel fuel in DI diesel engine modified by nozzle geometry. J. Energy Inst. 89 (4), 668–682.

Vijay Kumar, M., Veeresh Babu, A., Ravi Kumar, P., 2018. Experimental investigation on the effects of diesel and mahua biodiesel blended fuel in direct injection diesel engine modified by nozzle orifice diameters. Renew. Energy 119, 388–399.

Wong, K.I., et al., 2013. Modeling and optimization of biodiesel engine performance using advanced machine learning methods. Energ. 55, 519–528.

Wong, P.K., et al., 2015a. Modeling and optimization of biodiesel engine performance using kernel-based extreme learning machine and cuckoo search. Renew. Energ. 74, 640–647.

Wong, K.I., et al., 2015b. Sparse Bayesian extreme learning machine and its application to biofuel engine performance prediction. Neurocomputing 149 (Part A), 397–404.

Wu, S., Wang, Y., Cheng, S., 2013. Extreme learning machine based wind speed estimation and sensorless control for wind turbine power generation system. Neurocomputing 102, 163–175.

Yesilyurt, M.K., 2019. The effects of the fuel injection pressure on the performance and emission characteristics of a diesel engine fuelled with waste cooking oil biodiesel-diesel blends. Renew. Energy 132, 649–666.

Yuan, L.Z.a. J., 2015. Fault diagnosis of power transformers using kernel based extreme learning machine with particle swarm optimization. Appl. Math. Inf. Sci. 9, 1003–1010.